JOURNAL OF MATERIALS SCIENCE 9 (1974) · 1409–1419

Temperature effects in the fracture of PMMA

G. P. MARSHALL*, L. H. COUTTS, J. G. WILLIAMS
Mechanical Engineering Department, Imperial College, London, UK

Experiments are described in which the fracture toughness, K_c, of PMMA has been determined in the temperature range −190 to + 80° C and over the crack speed range of 10^{-2} to 10^{2} mm sec^{-1}. Single edge notch tension was used for instability measurements but the other data were obtained using the double torsion method. In the range −80 to +80° C the variations in K_c may be described in terms of modulus changes and a constant crack opening displacement criterion. Crack instabilities are correlated with isothermal-adiabatic transitions at the crack tip. Below −80° C there is an inverted rate dependence associated with thermal effects during post-instability crack propagation.

1. Introduction

There has been considerable effort devoted to the determination of accurate fracture toughness versus crack speed curves for polymers at room temperature. In particular, polymethylmethacrylate (PMMA) has been intensively studied and a review of all published data [1] showed that there is a consistent explanation for all the numbers given when the data are correlated as a function of crack speed. Data obtained at other temperatures are less plentiful and there is considerable variation between the results quoted by various authors [2-7]. Fig. 1 shows all the published data plotted as stress intensity factor, K_c, as a function of temperature. Some of these results have been obtained at instability and some at the onset of slow cracking (as shown), but even accounting for this, there is considerable difference in trends except that K_c tends to increase with decreasing temperature. It was considered worthwhile, therefore, to make precise measurement of K_c as a function of crack speed over the temperature range −190 to +80° C.

The published data are generally obtained on single edge notched (SEN) specimens or some form of cleavage test. At any temperature the form of curve to be expected is as shown in Fig. 2. Slow crack speeds give a rising K_c curve resulting in stable growth (I) until an instability is reached (II) after which it is not possible to achieve stability since K_c decreases with increasing $\dot{a}$ (III) until the rapidly rising curve associated with kinetic effects (IV) is reached. On an SEN specimen (see Fig. 3d) slow crack growth will start at some point in region (I), depending on the testing rate, and the crack will grow giving an increasing K_c until instability is reached (II). Crack initiation is identified by observing the onset of slow crack propagation with a microscope and K_c at initiation is calculated using the initial crack length. For the instability value of K_c, the maximum load is used and the crack length taken as the initial length plus the slow growth portion, which can easily be discerned on the fracture surface [8]. The initiation K_c would be expected to be rate dependent while the instability value would not. The determination of crack speeds ($\dot{a}$) at each K_c value is difficult with SEN specimens since K varies rapidly with crack length and, therefore, $\dot{a}$ changes rapidly.

To overcome this problem, parallel cleavage (PC) tests are often employed (see Fig. 3b) since the crack speed changes are much less. Indeed, a tapered cleavage (TC) specimen may be used (Fig. 3c) which is specifically contoured to give a constant speed for a constant load. This method has been used successfully on polymers [9] but it requires great practical skill because of variations in the crack geometry and is very time-consuming to use. A more convenient configuration

*Present address KC Research Limited, Cedar House, Wycombe Road, Prestwood, Bucks.

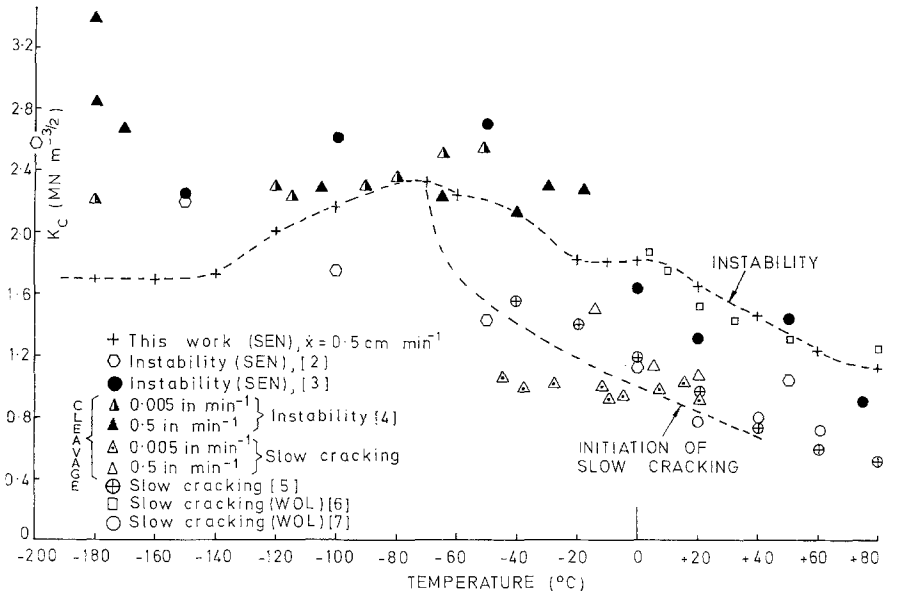

Figure 1 The comparison of published K_c values as functions of temperature. ◬ and △ are taken from [4].

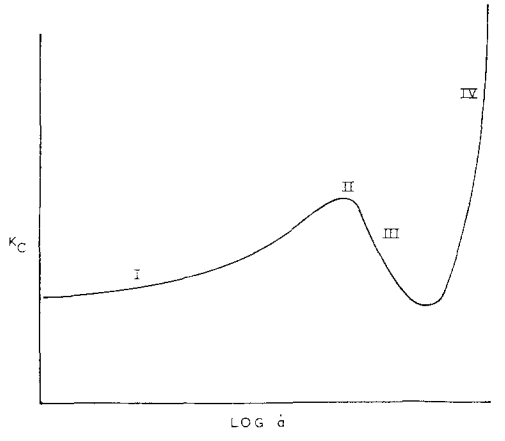

Figure 2 Schematic representation of K_c versus crack speed curve.

is that of double torsion (DT) (Fig. 3a) which also has a constant speed characteristic but is much more easily used, since it is not prone to crack wandering. This method has been employed here for determining the crack speed data although some cross-checks are included on TC specimens.

All the tests reported here were performed in a temperature cabinet designed to fit on an Instron testing machine with a cross-head rate range of 0.005 to 50 cm min^{-1}. The cabinet was well insulated thermally and temperatures could be controlled to $\pm$ 1°C. Above ambient

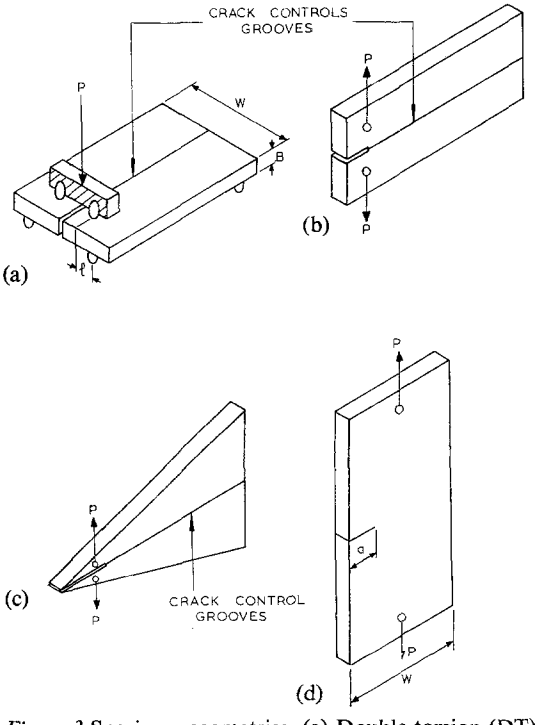

Figure 3 Specimen geometries. (a) Double torsion (DT); (b) parallel cleavage (PC); (c) tapered cleavage (TC); (d) single edge notch (SEN).

temperatures were achieved with bar heaters on the cabinet walls, and for low temperatures nitrogen gas was used to blow in liquid nitrogen

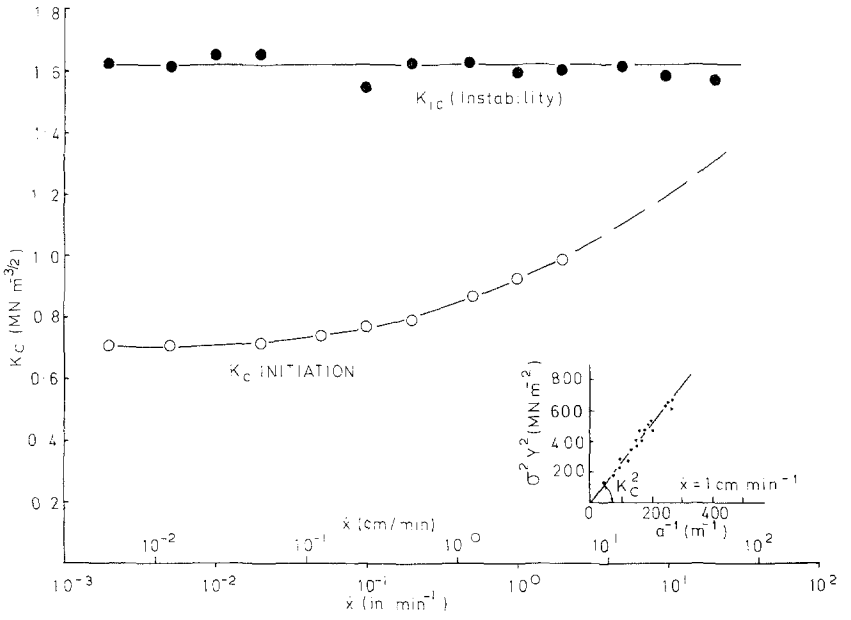

Figure 4 K_c at initiation and instability as a function of cross-head rate at 20° C from SEN tests.

and the vapour was circulated using a high speed fan. A controller, working from a thermocouple in the cabinet, controlled both the nitrogen flow and the bar heaters. Various door designs were employed to allow observation of the crack growth and arm holes were included to facilitate the changing of specimens. Crack speeds were recorded with a travelling microscope at low speeds and on a television system with video tape at higher speeds. A UV recorder was used instead of the normal load chart at the higher rates.

2. Single edge notch tests

The critical stress intensity factor K_c may be calculated for this geometry from the relationship

$$K_c = Y\sigma\sqrt{a} \tag{1}$$

where $Y = \sqrt{\pi}$ for an infinite plate. Finite width and free edge effects are included in [10] giving

$$Y = \left[1.99 - 0.41\left(\frac{a}{W}\right) + 18.7\left(\frac{a}{W}\right)^2 - 38.48\left(\frac{a}{W}\right)^3 + 53.85\left(\frac{a}{W}\right)^4\right]. \tag{2}$$

where a = crack length and w = specimen width (see Fig. 3d). Tests were performed at various cross-head rates at each temperature and the K_c value at initiation and instability determined by plotting $Y^2\sigma^2$ versus a^{-1}. Fig. 4 shows some data at 20° C, the initiation value is rate dependent and the instability value, as expected, is not. Fig. 5 shows the K_c values obtained in this way over the whole temperature range and between −70 to +80° C. An initiation value obtained at 0.5 cm min^{-1} is also shown and the two curves cross at approximately −80° C. There is a noticeable plateau in the instability results in the region −20 to 0° C and it is possible that this is due to freezing effects associated with absorbed water. Below −80° C there is a pronounced rate effect in the instability values and no initiation could be determined since no slow growth was observed. The most notable features of this region are the inverted strain-rate dependence in that the higher cross-head rate gives the lowest K_c value, and the tendency for the data to become independent of temperature below about −140° C.

The data are shown in Fig. 1 (the broken lines) and give a reasonable degree of agreement with those of other workers for temperatures > −80° C for both initiation and instability. Below −80° C, however, there is a much greater disparity. The amount of information available from such data is limited, however, and it is necessary to determine the K_c versus crack speed curves to obtain the complete picture.

3. Double torsion tests

This specimen may be analysed by the general

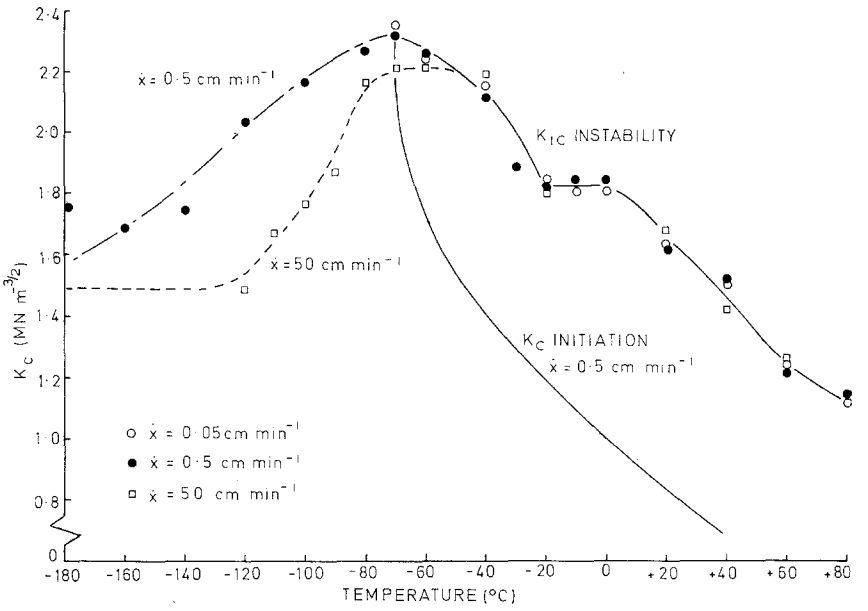

Figure 5 K_c at initiation and instability as a function of temperature from SEN tests.

compliance method [9],

$$K_c^2 = \left(\frac{p^2}{2B_c}\right)\left(E\frac{dC}{da}\right) \quad (3)$$

where p = the applied load, B_c = crack width (side grooving is usually employed so that $B_c \neq$ plate thickness B), E = modulus, and C = specimen compliance.

An approximate analysis gives an expression for C of the form

$$C = \left[\frac{6(1+\nu)l^2}{EWB^3}a\right] + C_0 \quad (4)$$

where C_0 = specimen compliance for $a = 0$, l = distance between loading points (see Fig. 3a), W = plate width, B = plate thickness, so that

$$E\frac{dC}{da} = \frac{6(1+\nu)l^2}{WB^3} \quad (5)$$

i.e. the product is independent of the modulus.

Since K_c and E are constant for a given crack speed and dC/da is a constant then p will also be constant. The crack speed ($\dot{a}$) for a cross-head rate ($\dot{x}$) is given by

$$\dot{a} = \frac{\dot{x}}{p(dC/da)} \quad (6)$$

i.e. a constant. The ratio $\dot{x}/\dot{a}$ may be re-expressed from Equation 3 as

$$\frac{\dot{x}}{\dot{a}} = \sqrt{\left(2B_c E\frac{dC}{da}\right)\left(\frac{K_c}{E}\right)}. \quad (7)$$

Specimens were manufactured with W = 80 mm, B = 6 mm and the loading system gave l = 27 mm resulting in a calculated calibration factor of

$$E\frac{dC}{da} = 3.3 \times 10^5\ \text{m}^{-2}.$$

Experiments were performed at various $\dot{x}$ values in the temperature range -60 to $+60$°C For each test the loads and crack speeds were

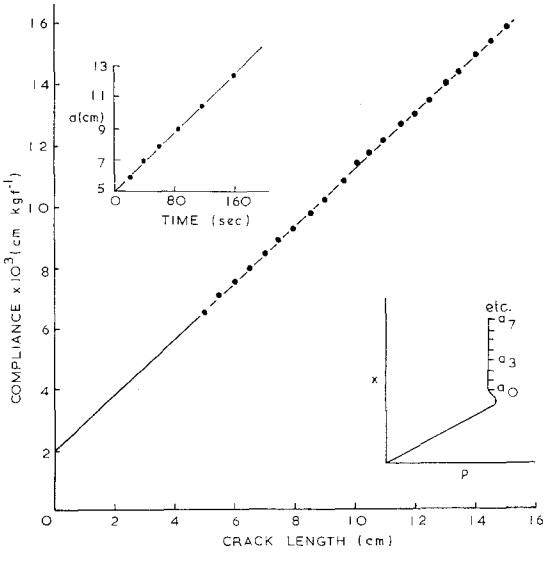

Figure 6 Double torsion calibration curves at 20°C and $\dot{x}$ = 0.10 cm min^{-1}.

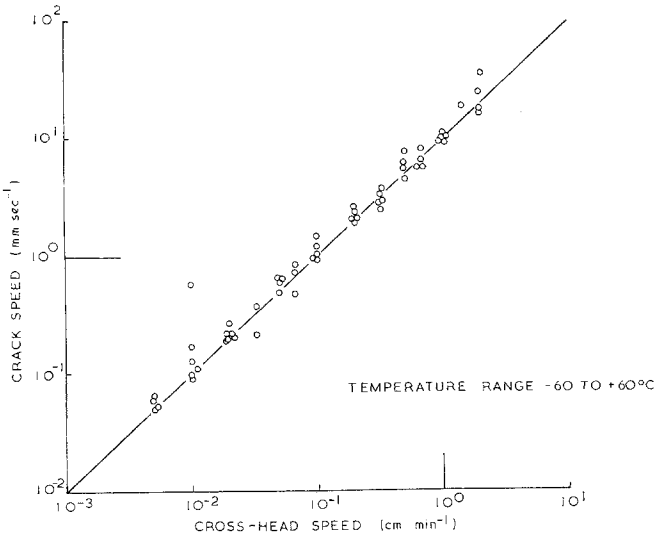

Figure 7 Crack speeds as a function of cross-head rate for various temperatures from the DT tests.

constant at any given rate and temperature as illustrated in Fig. 6. A complete compliance curve at 20°C is also given showing that dC/da is a constant and using E for this strain-rate (2900 MN m^{-2}) gives

$$E\frac{dC}{da} = 3.4 \times 10^5 \text{ m}^{-2},$$

which is essentially identical with the calculated value. Fig. 7 shows crack speeds measured at a wide range of cross-head speeds at several temperatures and the line is that for $\dot{a} \propto \dot{x}$, indicating (from Equation 7) that K_c/E is a constant over this whole range with a value of 3.2×10^{-4} m$^{\frac{1}{2}}$ (B_c = 4 mm).

A cross-check was made on the consistency of the DT method at 20°C by determining K_c from Equation 3 at a range of crack speeds and the results are shown in Fig. 8. A further series of tests had previously been performed using the TC method [9] and these results are also shown in Fig. 8. There is good agreement, demonstrat-

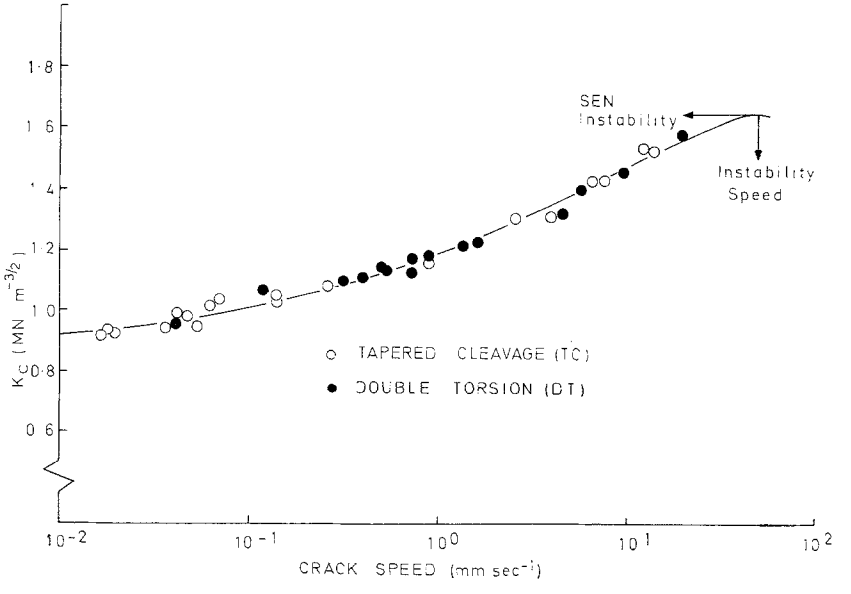

Figure 8 K_c as a function of crack speed at 20°C from DT and TC tests.

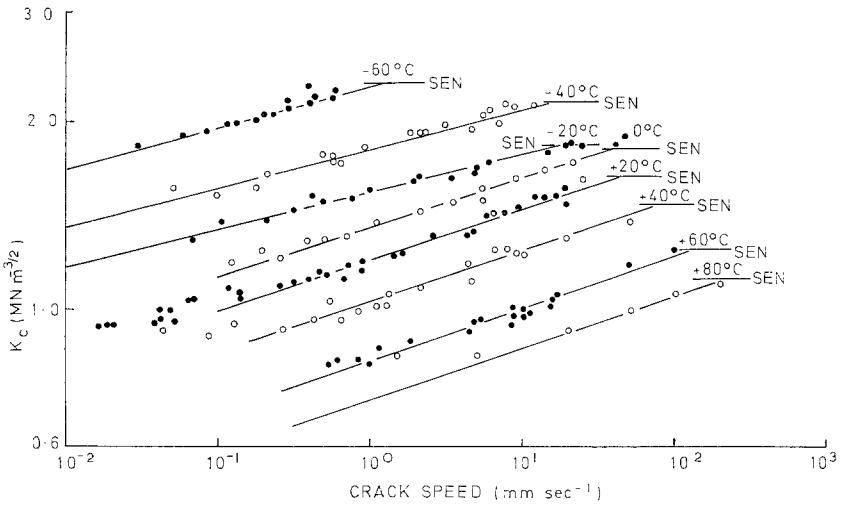

Figure 9 K_c as a function of crack speed at various temperatures – stable crack growth in DT tests.

ing the validity of the DT configuration. The highest crack speed shown is the limit for stable crack growth (i.e. $\sim$ 20 mm sec^{-1}) and extrapolating the curve to meet the SEN value (as shown in Fig. 8) indicates a true instability speed of 50 mm sec^{-1}. This method was used at all other temperatures to determine the instability speeds.

The data obtained in the range -60 to $+80$°C (the limits for stable crack growth and ductile tearing respectively) are shown in Fig. 9 as log K_c versus log $\dot{a}$ lines together with the SEN instability values. There is some tendency for the lines to decrease in slope at their lower extremities but in general the slope is constant at about 0.06. As the temperature decreases, the lines are displaced along the log $\dot{a}$ axis in accordance with an Arrhenius type equation giving an activation energy, H, of around 20 kcal mol^{-1}. This indicates that the PMMA β relaxation process is operating in this range and agrees with other published data [11].

The data are shown plotted as K_c as a function of temperature over the range -180 to $+80$°C

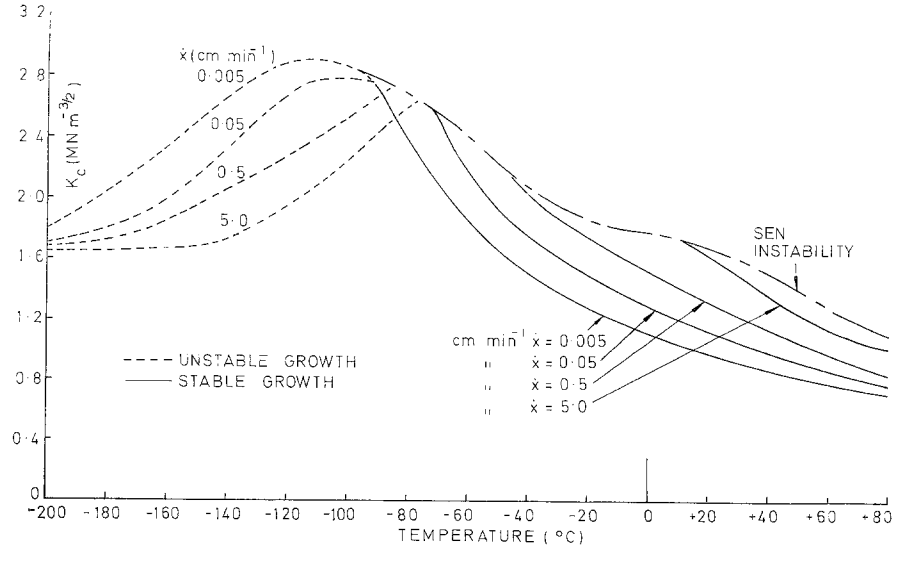

Figure 10 K_c as a function of temperature for various cross-head rates from DT tests.

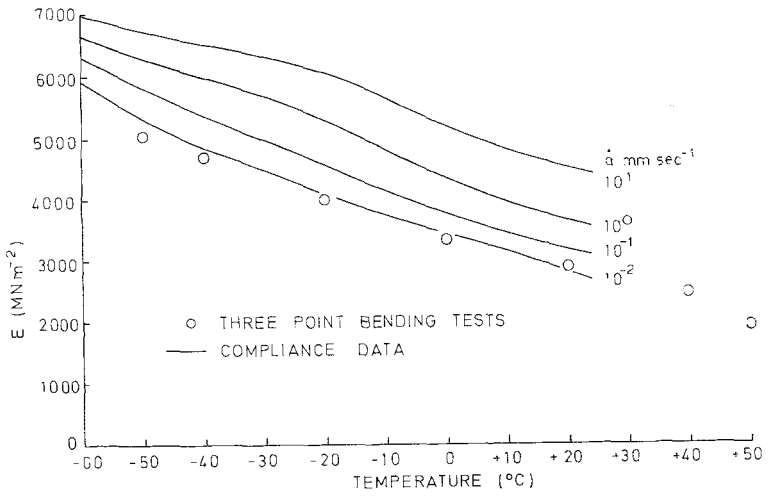

Figure 11 Modulus, E, as a function of temperature at various crack speeds from DT test compliance measurements.

in Fig. 10 with lines drawn at various $\dot{x}$ values. The pattern of stable growth behaviour for temperatures $> -80°C$ fits well with the SEN instability data and below $-80°C$ the same inverted rate dependence as with the SEN tests is apparent; the curves tending to converge at the lower temperatures.

Since the compliance may be determined at each temperature and crack speed and $E(dC/da)$ is a geometric factor, then E may be determined for all these conditions if one value is known. Fig. 11 shows E values determined in this way at various crack speeds. Some values obtained using three point bending are also shown and give the same trend. Again, a β process is indicated with $H = 20$ kcal mol^{-1} and a relationship between K_c and E is indicated. Fig. 12 shows K_c plotted against E over a range of crack speeds and temperatures and a constant ratio of $K_c/E = 3.1 \times 10^{-4}$ m$^{\frac{1}{2}}$ is obtained, agreeing closely with that obtained from crack speed measurements (Fig. 7).

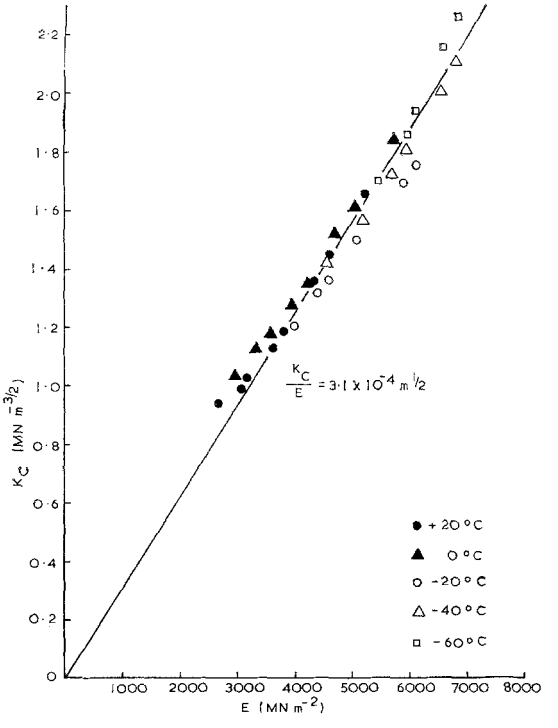

Figure 12 K_c as a function of E for various temperatures and crack speeds.

4. Discussion of the results

The deformation processes at the crack tip in a polymer may be modelled successfully by a Dugdale line plastic zone as shown in Fig. 13. [12]. For a non-work-hardening yield stress, σ_y, the zone length is given by

$$\Delta = \frac{\pi}{8} \cdot \frac{K_c^2}{\sigma_y^2} \tag{8}$$

and the displacement at the crack tip (the crack opening displacement or COD) is

$$u = \frac{K_c^2}{\sigma_y E} \tag{9}$$

providing that, in both cases, $\sigma < 0.5\,\sigma_y$. It has been shown [12] that the yield strain, e_y, is largely insensitive to both rate and temperature

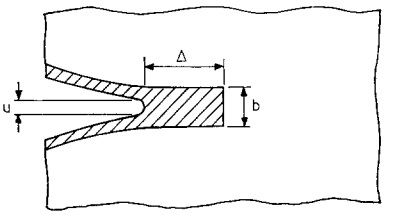

Figure 13 The Dugdale line zone at the crack tip.

in PMMA and the analysis may be considerably simplified by assuming that e_y is a constant and

$$\sigma_y = e_y E . \tag{10}$$

It will also be assumed here that the fracture criterion is a constant COD, u, which is also independent of both rate and temperature. From Equation 9 we have

$$K_c = \sqrt{(ue_y)}\, E . \tag{11}$$

This is consistent with the experimental finding for both crack speed and direct K_c and E measurements and

$$\sqrt{(ue_y)} \approx 3 \times 10^{-4}\ \mathrm{m}^{\frac{1}{2}} .$$

e_y may be taken as approximately 0.06 [12] so that $u \approx 1.6\ \mu$m – which is in reasonable accord with direct measurements. A constant u implies a constant Δ and from Equations 8 and 9 we have

$$\Delta = \frac{\pi}{8}\frac{u}{e_y} \approx 10\ \mu\mathrm{m} . \tag{12}$$

Correlations between K_c and E have been noted previously [13] over a more limited temperature range and interpreted as a fixed surface energy (i.e. K_c^2/E = constant). The time dependence of the modulus at any fixed temperature may be reasonably accurately represented by

$$E = E_0\, t^{-n} \tag{13}$$

where t = the time scale, E_0 = the unit time modulus, and $n = \mathrm{d}\ln E/\mathrm{d}\ln t$ and is assumed to be approximately constant.

The exponent n is a measure of the degree of time dependence acting (e.g. $n = 0$ for an elastic material) and corresponds to the loss factor tan δ. A simple comparison of a ramp wave form shows that tan $\delta \approx 0.88\, n$ for $n \ll 1$ and clearly, since the modulus changes were measured in the range -80 to $+80$°C where a distinct β transition occurs, tan δ (and hence n) would be expected to go through a peak within this range. There is some evidence in Fig. 9 of n decreasing at the lower rates and temperatures and the expected sigmoidal form could be inferred but not determined with any precision in this way. The values of n agree reasonably well with those of measured peak tan δ [11] values and the rate of variation is not expected to be great. However, the subsequent analysis, which is based on a constant n, will be inappropriate at extremes of rate or temperature as n tends to zero.

The time scale appropriate to the deformations at the crack tip may be deduced simply from the ratio [14],

$$t = \frac{\Delta}{\dot{a}}$$

but it is more precise to consider the elastic strain-rate around the crack tip and to assume that the strains are of the order e_y which gives,

$$t = \left(\frac{8}{\pi^2}\right)\left(\frac{\Delta}{\dot{a}}\right) . \tag{14}$$

The combination of Equations 11 to 14 gives the result

$$K_c = \sqrt{(ue_y)}\left(\frac{\pi e_y}{u}\right)^n E_0\, \dot{a}^n . \tag{15}$$

Since the temperature dependence may be described by the Arrhenius equation, the time t^1 at a temperature T may be computed from t at T_0 by,

$$t^1 = t\, \mathrm{e}^{-H/R(1/T - 1/T_0)} \tag{16}$$

so that the Equation 15 becomes,

$$K_c = \sqrt{(ue_y)}\left(\frac{\pi e_y}{u}\right)^n E_0\, \mathrm{e}^{nH/R(1/T - 1/T_0)}\, \dot{a}^n \tag{17}$$

and this is a reasonable representation of the data in Fig. 9 with $n = 0.06$ and $H/R = 10^4$ K.

The instabilities observed are of considerable practical significance and the controlling mechanism has been the subject of some recent debate. It has been suggested that the instability conditions correspond to a tan δ peak and are governed by the β process [4]. There is no evidence to support this in Fig. 9 since the instabilities do not occur at maximum n and the crack speed decreases much less rapidly with temperature than is required by the β transition. Fig. 14 shows some β transition data with the constant E and K_c taken from Figs. 9 and 11 as well as the instability points and it is clear that they are not governed by the same process.

The stability of crack growth in slow growth is governed by n since it is the increase in E with crack speed which makes the system stable. It

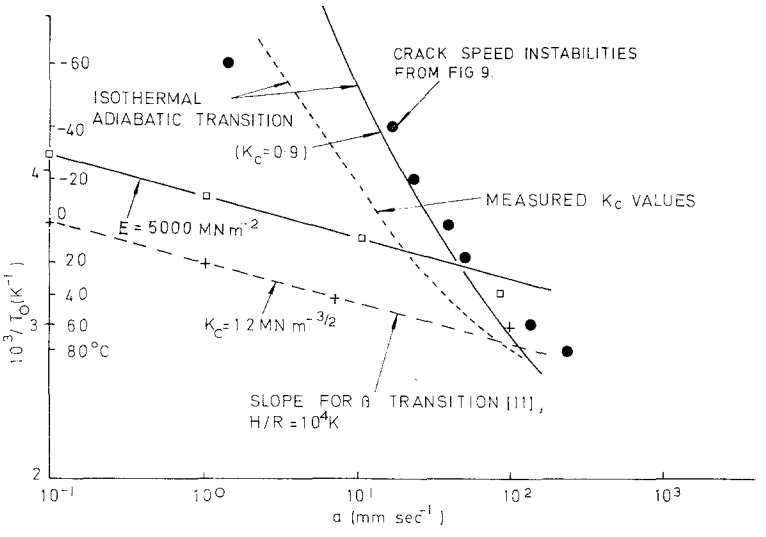

Figure 14 Crack speeds at instability.

would be expected, therefore, that the crack would be more, rather than less, stable at maximum n.

An alternative explanation for the instability is the onset of significant thermal softening in the crack tip region as the deformation changes from an isothermal process at low crack speeds to adiabatic at high speeds [15-17]. The low thermal conductivity of polymers makes the speeds rather lower for this effect than in metals and previous predictions on 20°C data showed good agreement [15—17] with experiment. The adiabatic temperature rise may be computed from the energy dissipated and the zone thickness b so that

$$\Delta\tilde{T} = \frac{\sqrt{(ue_y)}\,K_c}{\rho c b} \tag{18}$$

and ρ is the density and c the specific heat. The zone may be modelled as a parallel strip, embedded in an infinite medium, in which heat is generated at a constant rate, and the temperature rise for a time t is given by [18]

$$\Delta T = \Delta\tilde{T}\left[1 - 4i^2\,\mathrm{erf}\,c\sqrt{\left(\frac{b^2}{16\kappa t}\right)}\right] \tag{19}$$

where $\kappa = k/(\rho c)$ and k is the thermal conductivity. The convention i^2 erf c refers to the second integral of $(1 - \mathrm{erf}\ x)$ where erf x is the error function [18]. b is known to be small [17] and a useful lower bound to crack speed can be obtained by taking the limit as $b \to 0$ so that

$$\Delta T = \left[\frac{ue_yE}{\sqrt{(\pi\rho ck)}}\right]\left[\frac{1}{\sqrt{t}}\right] = \frac{e_y}{\sqrt{(\rho ck)}}K_c\sqrt{\dot{a}}\cdot \tag{20}$$

Previous solutions [17, 19] have used forms similar to this and then guessed some value for ΔT (e.g. 50°C for T_0 = 20°C) so that the instability speed would not be expected to be dependent on T_0. Equation 17, however, provides a method of determining ΔT since the condition for $dK_c/d\dot{a} = 0$ may be determined and is

$$\frac{dT}{d\dot{a}} = \left(\frac{R}{H}\right)\left(\frac{\bar{T}^2}{\dot{a}}\right) \tag{21}$$

where $\bar{T}$ is the temperature necessary for $dK_c/d\dot{a} = 0$.

Similarly, from Equation 20, we have a second condition for $dK_c/d\dot{a} = 0$ so that

$$\frac{dT}{d\dot{a}} = \left[\frac{e_yK_c}{\sqrt{(\rho ck)}}\right]\left[\frac{1}{2\sqrt{\dot{a}}}\right] \tag{22}$$

and combining Equations 20, 21 and 22 we have

$$\frac{2R}{H}\bar{T}^2 = \bar{T} - T_0\,. \tag{23}$$

Table I gives values for $\bar{T} - T_0$ together with values of $\dot{a}_c$ computed from Equation 20 using the following values:

$$\frac{H}{R} = 10^4\ \mathrm{K};\ e_y = 0.06;\ u = 1.6\ \mu\mathrm{m};$$
$$K_c = 0.9\ \mathrm{MN\ m^{-3/2}};\ \rho = 1.2\ \mathrm{g\ cm^{-3}};$$
$$k = 5 \times 10^{-5}\ \mathrm{cal\ (cm\,^\circ C\ sec)^{-1}}$$

TABLE I Calculated temperature rises and crack speeds at instability, together with experimental crack speeds

T_0 (°C)	$\bar{T}-T_0$ (°C)	$\dot{a}_c$ (mm sec^{-1})	Experimental $\dot{a}_c$ (mm sec^{-1})
80	29.2	126.4	240
60	25.7	92.4	140
40	22.5	66.5	85
20	19.5	46.8	50
0	16.8	32.4	40
−20	14.3	21.7	24
−40	12.0	14.0	17
−60	9.9	8.8	1.4

and a linear variation of c with T_0 is included since $\bar{T} - T_0$ is not large, namely,

$$([c = 1.2 \times 10^{-3} T_0 \text{ cal } (^\circ\text{C g})^{-1} (T_0 \text{ in K})] .$$

Fig. 14 shows these results and indicates a good agreement with the trend. $K_c = 0.9$ MN m$^{-3/2}$ was used since it is lower bound to the K_c values and the broken line is obtained with actual K_c values from Fig. 9. As expected the speeds are lower than the experimental results since $b = 0$ has been assumed but the trend is sufficiently good to assume that the controlling factor is an isothermal-adiabatic transition.

There is a more rapid decrease in the instability speed at −60°C than expected from the analysis and at −80°C no stable crack growth was achieved, indicating a speed of less than 10^{-2} mm sec^{-1}. It seems likely that these temperatures represent the lower end of the β transition region so that n is decreasing; eventually tending to zero around −100°C within the measurable crack speed range, so that stable crack growth is not possible. The rate dependence observed below −80°C is not thought to be visco-elastic in origin but to stem from thermal effects. The coupling of K_c, ΔT and $\dot{a}$ as expressed in Equation 20 gives a qualitative description of the results but numerical comparisons are difficult because $\dot{a}$ is not known for unstable crack growth. Support for this concept is provided by the observation of very substantial craze growth at the crack tip prior to fracture ($\sim$ 0.2 mm) indicating a much reduced yield stress. At the very low temperatures, the results tend to become independent of rate and it is possible that the temperature rise is reaching the adiabatic limit as expressed in Equation 18. These comments relating to very low temperatures apply equally to the very high crack speed region at higher temperatures, i.e. III in Fig. 3.

5. Conclusions

The observed fracture data in the temperature range −80 to +80°C is accurately modelled by assuming a Dugdale model at the crack tip and taking the crack opening displacement as a constant. The observed changes in K_c are shown to be reflections of changes of the modulus with rate and temperature and are largely governed by the β transition. The instabilities observed in the range −40 to +80°C appear to be due to thermal softening effects but below −40°C there is a suggestion that the visco-elastic effects arising from the β transition may cease to act, leading to an essentially elastic, and therefore unstable, material. Rate-dependence effects observed at temperatures as low as −180°C would appear to be due to thermal effects in post-instability behaviour but there is no quantitative support for this contention.

References

1. G. P. MARSHALL and J. G. WILLIAMS, *J. Mater. Sci.* **8** (1973) 138.
2. J. P. BERRY, *J. Polymer Sci.* **A1** (1963) 993.
3. P. L. KEY, Y. KATZ and E. R. PARKER, *Sci. Tech. and Aero. Rept.* (N68-29464) p. 2904 – NASA (UCRL-17911) (1968).
4. F. A. JOHNSON and J. C. RADON, *Eng. Fracture Mechs.* **4** (1972) 555.
5. L. J. BROUTMAN and F. J. MCGARRY, *J. Appl. Polymer Sci.* **9** (1965) 589.
6. J. J. BENBOW, *Proc. Phys. Soc. (London)* **78** (1961) 5.
7. N. L. SVENNSON, *Proc. Phys. Soc. (London)* **77** (1961) 876.
8. J. P. BERRY, *J. Appl. Phys.* **33** (1962) 741.
9. G. P. MARSHALL, L. E. CULVER and J. G. WILLIAMS, *Plastics and Polymers*, February (1969) 75.
10. H. F. BROWN and J. E. SRAWLEY, *A.S.T.M., S.T.P.* 410 (1966).
11. N. G. MCCRUM, B. E. READ and G. WILLIAMS, "Anelastic and dielectric effects in polymeric solids' (Wiley, New York, 1967).
12. J. G. WILLIAMS, *Int. J. Fracture Mechs.* **8** (1972) 393.
13. P. D. OLEAR and F. ERDOGAN, *J. Appl. Polymer Sci.* **12** (1968) 2563.
14. J. G. WILLIAMS and G. P. MARSHALL, to be published in *Proc. Roy. Soc.* (1974).
15. J. G. WILLIAMS, *Appl Materials Res.* April (1965) 104.
16. J. G. WILLIAMS, J. C. RADON and C. E. TURNER, *Polymer Eng. and Sci.* April (1968) 130.
17. R. P. KAMBOUR and R. E. BARKER JUN, *J. Polymer Sci.* **A2** (1966) 4.

18. H. S. CARSLAW and J. G. JAEGER, "Conduction of Heat in Solids", 2nd Edn (Oxford University Press, 1959).
19. N. LEVY and J. R. RICE, "Physics of Plasticity and Fracture" (M.I.T. Press, Cambridge, Mass., 1969-70).

Received 26 March and accepted 3 April 1974.